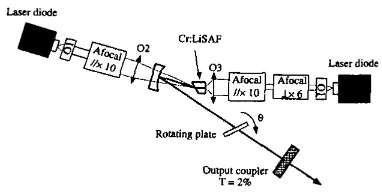

CFE6 Fig. 1 Experimental setup. The focal lengths of the objectives are respectively 15 mm, 100 mm, 60 mm for O1, O2 and O3. For the afocal systems: // (resp. ⊥) indicates that the afocal works in the direction parallel (resp. perpendicular) to the junction of the diode.

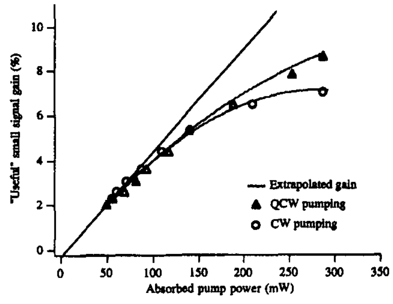

CFE6 Fig. 2 Small signal pass gain under different pumping configurations for one pumping diode. The "extrapolated gain" corresponds to a small signal gain without up-conversion process and without thermal quenching of fluorescence.

by polarization to the first one: the gain fell down to 4.8% principally due to quenching of fluorescence.

Then we decreased the thermal load by pumping the crystal with one diode at each side (Fig. 1). We obtained a higher value of g_0 equal to 10.2%. We used this last pumping configuration to produce nanosecond pulses. We added in the cavity an acousto-optic modulator to operate in a Q-switch regime. We obtained 7-μJ pulses with a duration of 230 ns at a repetition rate of 5 kHz at 850 nm. The energy per pulse remained above 5 μJ between 820 and 900 nm. The energy per pulse remained above 7 μJ up to 20-kHz repetition rate.

We are currently investigating a theoretical model describing the unsaturated gain that takes into account the influence of up-conversion and thermal quenching of fluorescence.

In conclusion, owing to *in situ* small signal gain measurement we succeeded in the realization of an efficient Q-switched diode-pumped Cr:LiSAF laser operating at high repetition rate (up to 20 kHz) producing tunable nanosecond pulses with an energy up to 7 μJ.

These works have been supported by the DRET, division optique under contract N°93/078.

1. M. A. Noginov, H. P. Jensen, A. Cassanho, in *Advanced Solid-State Lasers,* Vol. 15, OSA Proceedings Series (Optical Society of America, Washington, DC, 1993) pp 376–380.
2. S. A. Payne, L. K. Smith, R. J. Beach, B. H. T. Chai, J. H. Tassano, L. D. Deloach, W. L. Kway, R. W. Solarz, W. F. Krupke, Appl. Opt. **33**, 5526–5536 (1994).
3. M. Stalder, M. Bass, B. H. T. Chai, J. Opt. Soc. Am. B **9**, 2271–2273 (1992).

CFE7 **9:45 am**

Alexandrite laser passive Q-switching and spectral output enhancing up to 0.7 ÷ 1.15 μm

S. B. Mirov, A. Yu. Dergachev, V. B. Fleurov, V. A. Konyushkin,* *The University of Alabama at Birmingham, Department of Physics, 310 Campbell Hall, 1300 University Boulevard, Birmingham, Alabama 35294-1170*

The nature of the absorption band at 780 nm (at 300 K) in radiationally colored LiF crystals was investigated. It was shown that this absorption band formed under thermal annealing of LiF:F_3^- crystals completely coincides with the absorption band of N_1^- centers that were created by recharging of the neutral N_1 centers under low-temperature electron reirradiation of the LiF crystal.

The described LiF:N_1^- crystals are very promising as passive Q-switches and mode-lockers for alexandrite laser resonators. N_1^- centers feature a very high thermostability at temperatures up to 200°C and their absorption bands ideally match spectral emission of tunable alexandrite laser. Moreover, because of short lifetime of their excited level (determined only by a strong nonradiative decay), LiF:N_1^- crystals can serve as classical passive mode-lockers for the alexandrite laser resonators.

The nonlinear saturation properties of three color-center crystals (LiF:N_1^-, LiF:F_3^- and NaF:F_2^{+*}), promising for the alexandrite laser resonator passive Q-switching and mode-locking have been experimentally investigated. The induced-transparency measurements were performed using an electro-optic Q-switched unfocused alexandrite laser radiation at 775 nm with a pulse duration of about 100 ns. Figure 1 shows the internal transmission as a function of the 775-nm pump-power density. The induced-transmission measurements were analyzed using a four-level, fast-relaxing absorber model and the absorption cross sections of the crystals in the maxima of the absorption bands were estimated as follows: $\sigma_{\lambda=800nm}$ (LiF:F_3) = 7.7×10^{-17} cm^2; $\sigma_{\lambda=730nm}$ (NaF:F_2^{+*}) = 2×10^{-17} cm^2; LiF:N_1^- crystal exhibit a very high magnitude of absorption cross section $\sigma \geq 10^{15}$ cm^2 at λ = 775 nm.

We have demonstrated an efficient, high-performance passive Q-switching for the alexandrite laser utilizing LiF:N_1^- crystal yielding 50-mJ pulses of 80-ns (FWHM) pulse duration with efficiency (with respect to the free-running oscillation) of about 50%.

In addition to passive Q-switching of alexandrite laser we performed the experiments on the enhancing of its spectral range of tunability by utilizing LiF crystals with F_2^{+*} stabilized color centers. These F_2^{+*} centers exhibit a wide absorption band with λ_{max} = 630 nm with a half width of about 3500 cm^{-1} that overlaps with the alexandrite laser emission band (700–820 nm).

For the first time, to our knowledge, a room-temperature stable operation of the LiF:F_2^{+*} crystals pumped by the radiation of the alexandrite laser (740 nm) was realized in the region 0.82–1.15 μm with average output power of 0.7 W and efficiency of about 15%. The alexandrite color-center laser combination operated without a visible decrease in the output power at a pumping power density of about 50 MW/cm^2.

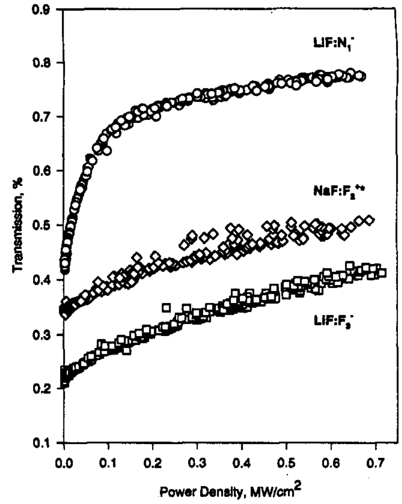

CFE7 Fig. 1 Induced transmission versus power density at 775 nm.

General Physics Institute, Vavilov str, 38, Moscow, 117333, Russia

CFF **10:30 am**
Room B1

Wave Mixing and Solid-State Lasers

D. D. Nolte, *Purdue University, Presider*

CFF1 **10:30 am**

Using tensor properties of four-wave mixing in semiconductor optical amplifiers for polarization-independent wavelength conversion or pump suppression

Roberto Paiella, Guido Hunziker, Jianhui Zhou, Kerry J. Vahala, Uzi Koren,* Barry I. Miller,* *Department of Applied Physics, Mail Stop 128-95, California Institute of Technology, Pasadena, California 91125*

Wavelength conversion by four-wave mixing (FWM) in semiconductor optical amplifiers (SOAs) has several advantages, including transparency to the modulation format and bit rate. An important feature of the intensity and polarization of the FWM wavelength-converted signal is their dependence on the polarizations of the input signal and pump waves. In this paper, we discuss the polarization properties of the FWM susceptibility χ_{ijkl} of strained multiple quantum well SOAs and their potential for application to polarization-independent wavelength conversion and pump suppression.

The nonlinear process described by χ_{ijkl} can be viewed as a two-step process as follows. Beating of the kth component of the pump and the lth component of the input signal induces dynamic gain and index gratings in the SOA. A converted signal along the ith direction is then generated through scattering of the jth component of the pump from these gratings. Here, we focus on FWM by carrier-density modulation and carrier heating, and show that the only nonzero components of χ_{ijkl} are those with $k = l$ and $i = j$. Physically, this implies that the dynamic gratings are only induced by beating of equal components of the pump and input signal (either both TE or both TM), and the TE (TM) component of the pump can be scattered into a converted signal only along the TE (TM) direction. The converted signal field at the SOA output can then be expressed in terms of the input signal and pump fields E^q and E^p through a second-rank tensor M_{ik} as follows,

$$E^s_i(L) = E^p_i(0) \sum_{k=1}^{2} M_{ik} E^q_k(0) E^p_k(0)^*. \quad (1)$$

This expression was experimentally verified by measuring the FWM conversion efficiency for different combinations of the input signal and pump polarizations. The experimental setup and the SOA used in these measurements are described in Refs. 1 and 2 respectively. The result of one such measurement is shown in Fig. 1, where we plot conversion efficiency versus angle of input signal polarization for a linearly polarized pump at $-45°$ and 30° relative to the growth axis. Also shown in the figure is a theoretical fit based on Eq. (1). Notice that, unlike in the case of a perfectly isotropic medium, the conversion efficiency is finite even for orthogonally polarized input waves. We then use this result to discuss condition for the realization of FWM wavelength conversion with efficiency independent of the input signal polarization.

As a second application, we propose and demonstrate a novel scheme for suppressing the pump wave from the SOA output. Given full knowledge of the matrix elements M_{ik}, one can set the input polarizations so that the converted signal polarization is orthogonal to that of the output pump. The pump can then be eliminated simply using a polarizer. We demonstrate this idea in Fig. 2, where the peaks shown are, from left to right, input signal, pump, and converted signal. The upper scan was taken directly at the SOA output, whereas for the middle scan a polarizer at the converted signal polarization was placed between the SOA and the detection stage; the pump is suppressed by more than 30 dB, while the signal is unaffected. These results also show how the model presented here can be used to control the polarization of the FWM signal, which is of importance in optical switching applications.

AT&T Bell Laboratories, Holmdel, New Jersey 07733

1. J. Zhou, N. Park, J. W. Dawson, K. J Vahala, M. A. Newkirk, B. I. Miller, IEEE Photon. Technol. Lett. 6, 50–52 (1994).
2. M. A. Newkirk, B. I. Miller, U. Koren, M. G. Young, M. Chien, R. M. Jopson, C. A. Burrus, IEEE Photon. Technol. Lett. 4, 406–408 (1993).

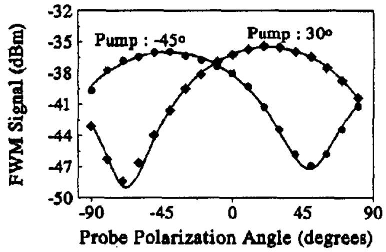

CFF1 Fig. 1 Converted signal power as a function of angle of linear polarization of the input signal relative to the TM direction, for linearly polarized pump at $-45°$ and $+30°$, and 1.5 nm detuning. The continuous lines are a fit to the magnitude squared of E_s as given by Eq. (1), with fitting parameters M_{ik}.

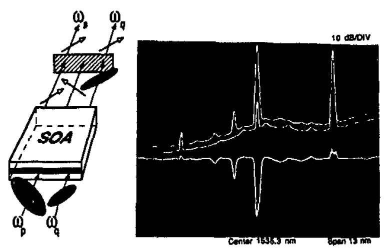

CFF1 Fig. 2 (left panel): illustration of our proposed pump suppression scheme: the input signal and pump polarizations are chosen so that, at the SOA output, the converted signal and pump are linearly polarized at +45° and $-45°$, respectively. (right panel): SOA output spectrum with the above input polarizations and 4 nm detuning, before (upper trace) and after (middle trace) a linear polarizer at +45°. The pump (center peak) is suppressed by more than 30 dB by the polarizer, whereas the converted signal (left peak) is essentially unattenuated. The lower trace is the ratio of the upper two.

CFF2 **10:45 am**

Four-wave mixing in semiconductor laser amplifiers: phase matching in configurations with three input waves

S. Diez, R. Ludwig, E. Patzak, H. G. Weber, G. Eisenstein,* R. Schimpe,**
Heinrich-Hertz-Institut für Nachrichtentechnik, Einsteinufer 37, D-10587 Berlin, Germany

Four-wave mixing (FWM) in semiconductor laser amplifiers (SLA) is of interest for both theoretical and experimental investigations. Considerable progress has been made towards a better understanding of the basic physical phenomena,[1–3] as well as towards applications for fast optical signal processing.[4,5] Conventional FWM experiments use a pump wave E_1 (frequency ω_1) and a signal wave E_A (ω_A) copropagating with the pump. To efficiently create mixing products, both waves are required to have the same polarization, which is a major drawback for the application of FWM in optical communication networks.

The addition of a second pumpwave E_2 (ω_2) allows for both, polarization-independent frequency conversion[4,6] as well as investigations on phase matching in optical amplifiers (for experimental setup see Fig. 1). Being mediated by various dynamic processes such as carrier-density pulsations (CDP), carrier heating (CH) and spectral hole burning (SHB), the beating of both pump waves causes a modulation of the gain medium with $\Delta\omega_{12} = \omega_2 - \omega_1$. This generates gain and index gratings (grating period $2\pi c/n\Delta\omega_{12}$), which create additional waves at frequencies $\omega_1 - \Delta\omega_{12}$, $\omega_2 + \Delta\omega_{12}$ and $\omega_A \pm \Delta\omega_{12}$. Figure 2 shows a schematic output spectrum, which is expected for E_1, E_2 and E_A having the same polarization. The generated spectral components E_B and E_C are frequency-converted replica of the signal wave and are almost independent of the polarization of E_A if $|\omega_A - \omega_{1,2}| >> |\Delta\omega_{12}|$.

In our experiments we used a polarization-insensitive bulk InGaAsP-SLA. Optical powers were measured by an optical spectrum analyzer (OSA). By exchanging the source for E_A and the OSA,

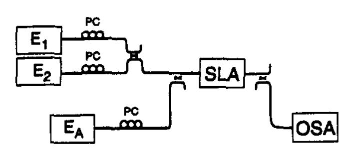

CFF2 Fig. 1 Schematic experimental setup for FWM with two pump waves E_1 and E_2 and a signal wave E_A. All optical signals are cw and are provided by external-cavity lasers. Polarization controllers (PC) allow for separate adjustment of the polarization for each wave. SLA-input powers were $P_1(0) = P_2(0) = 1.66$ mW and $P_A(0) = 0.16$ mW. The wavelength of E_2 was fixed at $\lambda_2 = 1564$ nm whereas λ_1 was tunable. The signal wavelength was chosen to be $\lambda_A = 1555$ nm.